Aquatic Mammals 2015, *41*(4), 444-454, DOI 10.1578/AM.41.4.2015.444

The Impact of Ocean Sound Dynamics on Estimates of Signal Detection Range

Jennifer L. Miksis-Olds,[1] Julia A. Vernon,[1] and Kevin D. Heaney[2]

[1]*Applied Research Laboratory, The Pennsylvania State University, State College, PA 16804, USA*
E-mail: jlm91@arl.psu.edu
[2]*OASIS Inc, 11006 Clara Barton Drive, Fairfax Station, VA 22039, USA*

Abstract

This work examines the impact of the dynamic soundscape on estimates of the signal detection area (DA) of passive acoustic monitoring stations. The range of signal detection was investigated at three site locations of the Comprehensive Nuclear-Test-Ban Treaty Organization International Monitoring System (CTBTO IMS). Transmission loss to each hydrophone was computed using the OASIS Peregrine parabolic equation model for a source within the upper 300 m of the water column to be consistent with the hypothesized location of vocalizing baleen whales. Seasonal, monthly, and daily soundscape measurements were incorporated into the sonar equation to estimate the variability in signal DA as a function of sound level and time. As a comparison, the seasonal analysis was repeated with a constant noise level to quantify the extent of variability due solely to changes in the seasonal sound speed profile. The greatest DA variability was observed at the Wake Island location in the Pacific Ocean where only a maximum of 18% of the 71 to 85% difference in DA estimates across seasons was attributable to changes in the sound speed profile. Differences in the daily DA estimate distributions as a function of frequency and location illustrate the impact of local sound field dynamics on the overall soundscape and the resulting signal detection range.

Key Words: soundscape, signal detection, active acoustic space, noise level

Introduction

Sound is capable of propagating over great distances in the ocean, and loud, low-frequency sources can propagate halfway around the globe (Heaney et al., 1991; Munk et al., 1994). For this reason, sound can be used to observe a variety of sources in marine ecosystems ranging from natural phenomena to anthropogenic activities. Ocean sound is also important to humans for tasks related to signal detection associated with military surveillance and environmental monitoring of animals for mitigation and regulatory purposes. Effective sound transmission in the marine environment is impacted by many factors, including physical and chemical properties of the sea water, as well as human-generated noise linked to ocean transportation, energy exploration, and military operations (Boyd et al., 2011). With the rising interest in the effect of human sound sources on the marine environment, passive acoustic monitoring (PAM) has become a valuable tool for detecting the presence of vocalizing animals (Mellinger et al., 2007). This work was designed to illustrate the operational significance a changing soundscape can have on the sampling area and the ultimate effectiveness of passive acoustic sensors.

The soundscape concept has recently been introduced to the field of underwater acoustics in an effort to capture and present the dynamic spatio-spectral-temporal aspects of an acoustic habitat related to contributions from biotic, abiotic, and anthropogenic sources (Slabbekoorn & Niels, 2008; Pijanowski et al., 2011; Van Opzeeland & Miksis-Olds, 2012; McWilliam & Hawkins, 2013; Staaterman et al., 2014). Understanding the complex cumulative and synergistic contributions underlying the variations in underwater soundscapes is a necessary first step in relating the impact of changes in the environmental sound levels to signal detection and, ultimately, to effective communication and masking of marine animals using sound. Studies have been conducted using aspects of the soundscape to estimate active acoustic space for vocalizing cetaceans, acknowledging the complexity in the environmental and biological parameters contributing to those estimates (Janik, 2000; Clark et al., 2009). Janik (2000) used single values from previously published noise level (NL) data under two different sea states, whereas Clark et al. (2009) used a

single parameter measurement of the 5th percentile for NL over time to estimate active acoustic space. This work aims to demonstrate how much the signal detection area (DA), or acoustic area covered by a single sensor or system, of a receiver varies as a function of soundscape over time. We do not attribute any biological relevance to the changes in DA due to changes in soundscape, rather we highlight the changes in DA because of the critical role this factor plays in accurate mitigation and monitoring of marine mammals using passive acoustic systems. Herein, we consider only the physical contributions to the soundscape and calculations of signal DAs (NL, transmission loss [TL], and source level [SL]) without accounting for the biological characteristics of hearing needed to extend the DA estimates to estimates of active acoustic space for communication. We have examined variability of the soundscape and its impact on DA at three time scales (seasonal, monthly, and daily) and five frequency bands up to 100 Hz. Three time scales of analysis were selected in order to provide operational relevance of the results to the PAM systems used to address monitoring questions at scales ranging from days to years.

Methods

Signal detection areas around Comprehensive Nuclear-Test-Ban Treaty Organization International Monitoring System (CTBTO IMS) stations at Diego Garcia (H08: Indian Ocean), Ascension Island (H10: Atlantic Ocean), and Wake Island (H11: Pacific Ocean) (Figure 1) were estimated using the passive sonar equation (Urick, 1967; Ainslie, 2010), written in Equation 1:

$$SE = SL - TL - NL - DT + DI + PG$$

A constant source level (SL) of 180 dB re 1 µPa was used to be reflective of the range of estimated blue and fin whale vocalization SLs (Širović et al., 2007; Clark et al., 2009; Samaran et al., 2010; Castellote et al., 2011). The loss due to range-dependent propagation is the transmission loss (TL). For this work, the directivity index (DI) and processing gain (PG) were set to zero, which is likely an underestimate of the performance for marine mammals that were communicating. The detection threshold (DT) was set so that a false alarm rate of 5% was achieved, meaning that for the local ambient noise time window, only 5% of the NLs exceeded this level.

Figure 1. Locations of each CTBTO IMS site used in this study. Each site contains two triads of hydrophones: one triad deployed to the north and one triad deployed to the south of each island location. A single northern and single southern hydrophone from each triad was used in this study.

DA was then computed by estimating the maximum range along each bearing for which the signal excess (SE) falls below zero. The TL for each season at each location was modelled along 360 bearings at 1° resolution using the OASIS Peregrine parabolic equation model for a receiver in the deep sound channel and a source position extending over the upper 300 m of the water column to be consistent with the hypothesized depth of vocalizing baleen whales (Oleson et al., 2007; A. K. Stimpert, pers. comm., 7 January 2015). The exact receiver depth varied from hydrophone to hydrophone to achieve placement in the deep sound channel (600 to 1,400 m depending on location). Peregrine is based on Michael Collins' (1993) split-step Padé PE marcher (RAM), a widely used acoustic model for low- to mid-frequency range dependent undersea sound propagation modelling. Starting from Collins' *RAMGEO 1.5* Fortran code, Peregrine has been ported to C, refactored for performance on modern computers, optimized for fully range-dependent problems, and is able to interpolate directly from geographically defined ocean field and bathymetry inputs. Monthly sound speed profiles were obtained from *The World Ocean Atlas* (https://www.nodc.noaa.gov/OC5/indprod.html). The bathymetry was taken from the global bathymetry database ETOPO1 (Amante & Eakins, 2009). Surface loss was negligible due to the low frequency of signals. Sea floor parameters of soft sand sediment were used, representing a global average of deep ocean sediment. Details of the geoacoustic parameters in the specific regions are not known and should not affect propagation in these environments due to direct path/sound channel propagation.

NL was calculated from acoustic recordings from a single north and south hydrophone at each CTBTO IMS monitoring location (see Lawrence, 2004, and Miksis-Olds et al., 2013, for details on CTBTO IMS monitoring stations and recording characteristics). NL measurements were made over three targeted 20-Hz bands (10 to 30 Hz, 40 to 60 Hz, and 85 to 105 Hz, respectively) and are reported as spectral levels in decibels (dB re 1 μPa^2/Hz). The 20-Hz band frequencies were selected to coincide with the dominant frequencies of blue and fin whale vocalizations (10 to 30 Hz) (Watkins et al., 1987; Stafford et al., 2004; Samaran et al., 2010), seismic airgun signals (40 to 60 Hz) (Tolstoy et al., 2004), and long-distance shipping (85 to 105 Hz) (Arveson & Vendittis, 2000; Ross, 2005) with the understanding that none of the frequency spectra of the identified sources are constrained to a single 20-Hz band and often span the full frequency spectrum of the recordings (< 1 to 125 Hz). Mean spectral levels were calculated using a Hann windowed 15,000 point Discrete Fourier Transform with no overlap to produce sequential 1-min power spectrum estimates over the duration of the dataset. Signal detection areas were estimated at three temporal scales—seasonal, monthly, and daily over 30 d. Seasonal estimates were derived from 2011 and are reflective of northern hemisphere seasons: Winter – January-March, Spring – April-June, Summer – July-September, and Fall – October-December. Monthly calculations were made over a 2-y period from 2010 to 2011, and daily estimates were made for November 2011. The 1-min power spectrum values were pooled to determine the 5% false alarm rate NL at each of the three time scales considered. This resulted in a single value NL for each day, month, and season to be used in the DA modelling. Detection range estimates were calculated from the maximum range along each bearing for which SE > 0 in each frequency category. Straight lines were used to connect the range points along the 360 bearings to form a polygon, and the area within the polygon was calculated from the bearing range lengths (Figure 2).

The DA_{max} is reflective of the DA estimate within a specific temporal analysis (seasonal, monthly, daily) that produced the greatest DA. The DA_{min} reflects the minimum DA estimate within each temporal analysis. In order to assess the relative importance of changing environmental sound levels, we define the % Difference for each temporal analysis as the % Difference between the maximum and minimum detection ranges (Equation 2):

$$\%\ Difference\ DA = \left(1 - \frac{DA\ Min}{DA\ Max}\right) * 100$$

A final seasonal analysis was conducted in 2011 at each site where the NL was set as a constant for all seasons. This was done to quantify the extent of variability due to changes in the seasonal sound speed profile alone. The % Difference across the year was calculated using Equation 2.

Results

Due to a discrepancy between the hydrophone depth and local bathymetry databases, signal detection ranges were not computed for the H10 North (N1) location at Ascension Island in the Atlantic Ocean. This impacted the DA analyses, so H10 N1 is not reflected in DA results. The NL data at this location was not affected, and H10 N1 is included in NL analyses and results. Effort is currently underway to resolve the H10 N1 depth discrepancy with CTBTO personnel. The

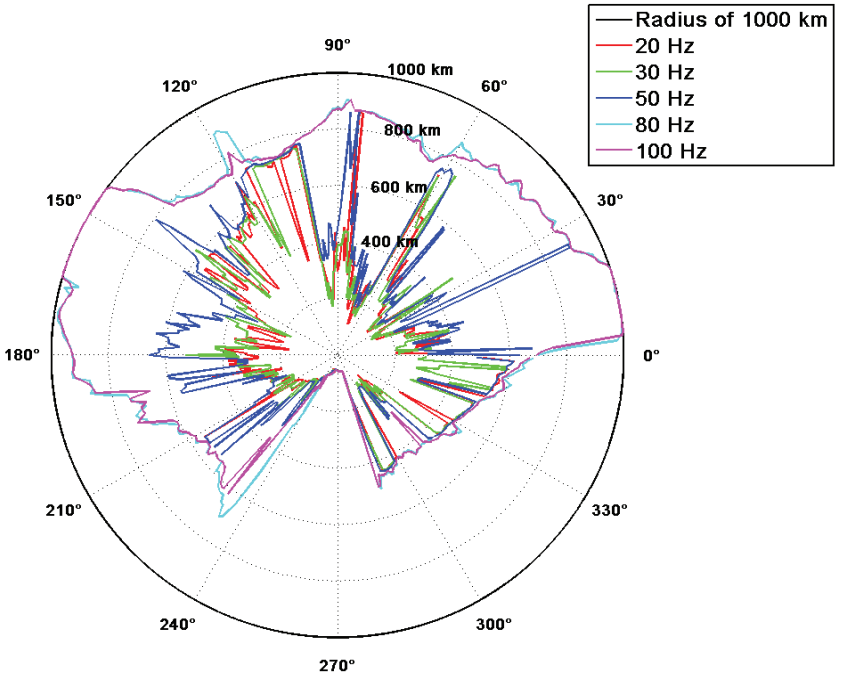

Figure 2. Full 360° signal DA from H08 N1 Diego Garcia North in the Indian Ocean for 2 November 2011; the DA was modelled out to 1,000 km for the five specified frequencies.

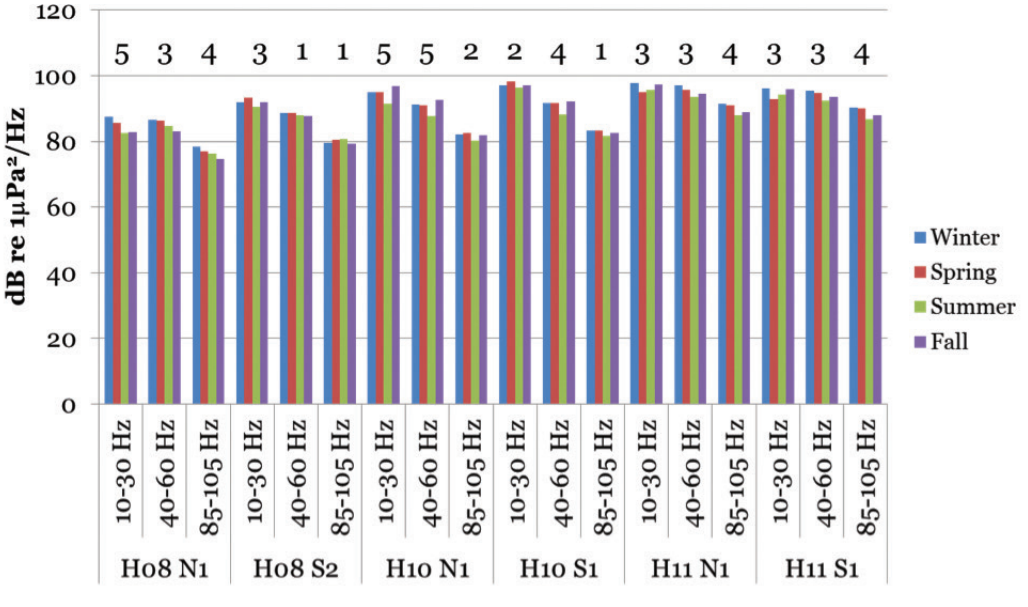

Figure 3. Seasonal noise levels (NLs) reflective of a 5% false alarm detection rate for each location and frequency band; numbers above each frequency band indicate the dB difference across seasons for that frequency band and location.

hydrophone depths and local bathymetry databases were verified for all remaining sites.

Seasonal NLs varied from 1 to 5 dB across frequency band and location, with the greatest seasonal NL variation (5 dB difference) recorded at H08 N1 Diego Garcia North and H10 N1 Ascension Island North (Figure 3). NL was greatest in winter (January-March) at H08 N1 Diego Garcia North and in fall (October-December) at H10 N1 Ascension Island North. Conversely, NL was lowest during the summer at these two sites. This corresponded to a 9 to 88% difference in signal DA at H08 N1 Diego Garcia North and 7 to 59% difference at H08 S2 Diego Garcia South (Figure 4) with summer and fall (July-December) having the largest DAs. The soundscape variability at H10 S1 Ascension Island South resulted in a 23 to 76% difference in DA estimates, and the largest DAs were observed in the austral winter (July-September). The greatest seasonal variability in DA due to soundscape was observed at H11 Wake Island with a 71 to 83% difference across frequency and hydrophone locations (Figure 4). DAs were consistently largest during the spring and summer (April-September) at Wake Island. The smallest DAs were observed in winter (January-March).

To isolate the seasonal dependence of the ocean temperature field on acoustic propagation, the seasonal DA estimates were computed for each location and signal frequency using a constant NL. This resulted in seasonal DA differences of 2 to 13% across frequencies at H08 Diego Garcia, 1 to 4% at H10 Ascension Island, and 0 to 19% at H11 Wake Island. The greatest seasonal variability due solely to changes in the seasonal sound speed profile was observed at Wake Island, which accounted for less than 20% of the observed variability in DA. Seasonal sound speed changes had little impact on the DA variability at H10 Ascension Island at any frequency, and the maximum amount of DA variability across modelled

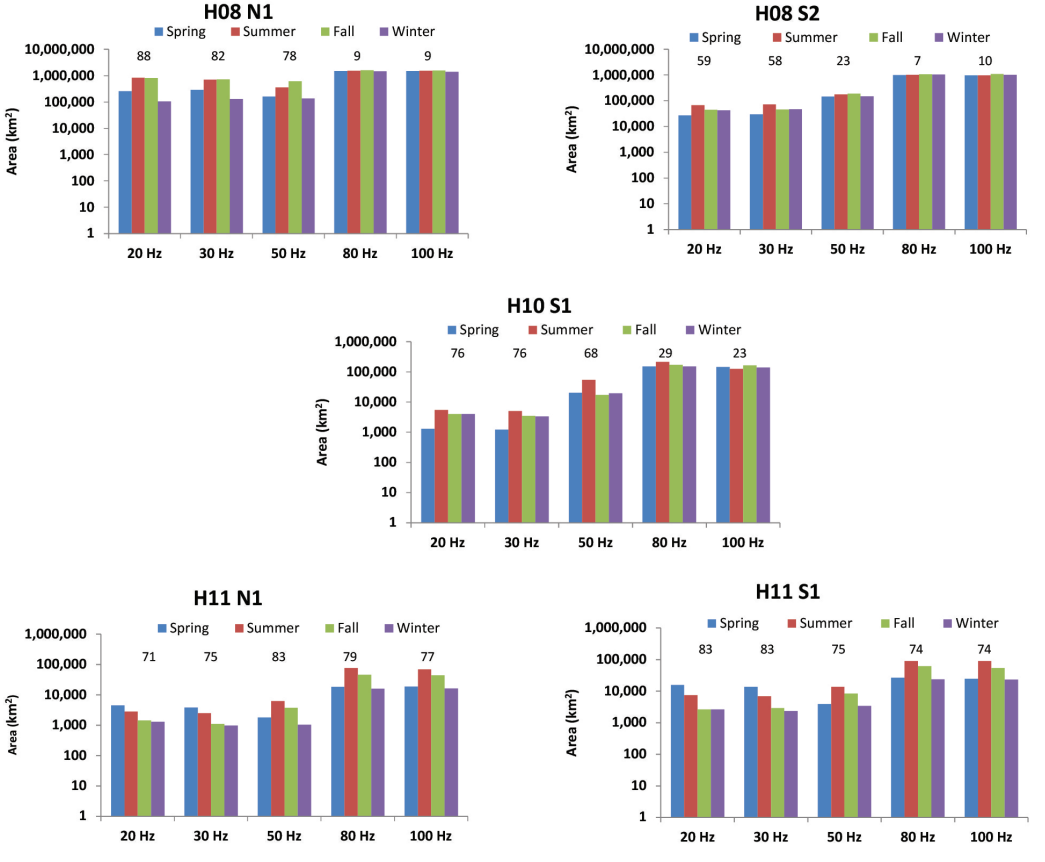

Figure 4. Seasonal DA estimates for the five modelled frequencies. Numbers above each frequency band indicate the % Difference across seasons for that frequency band and location.

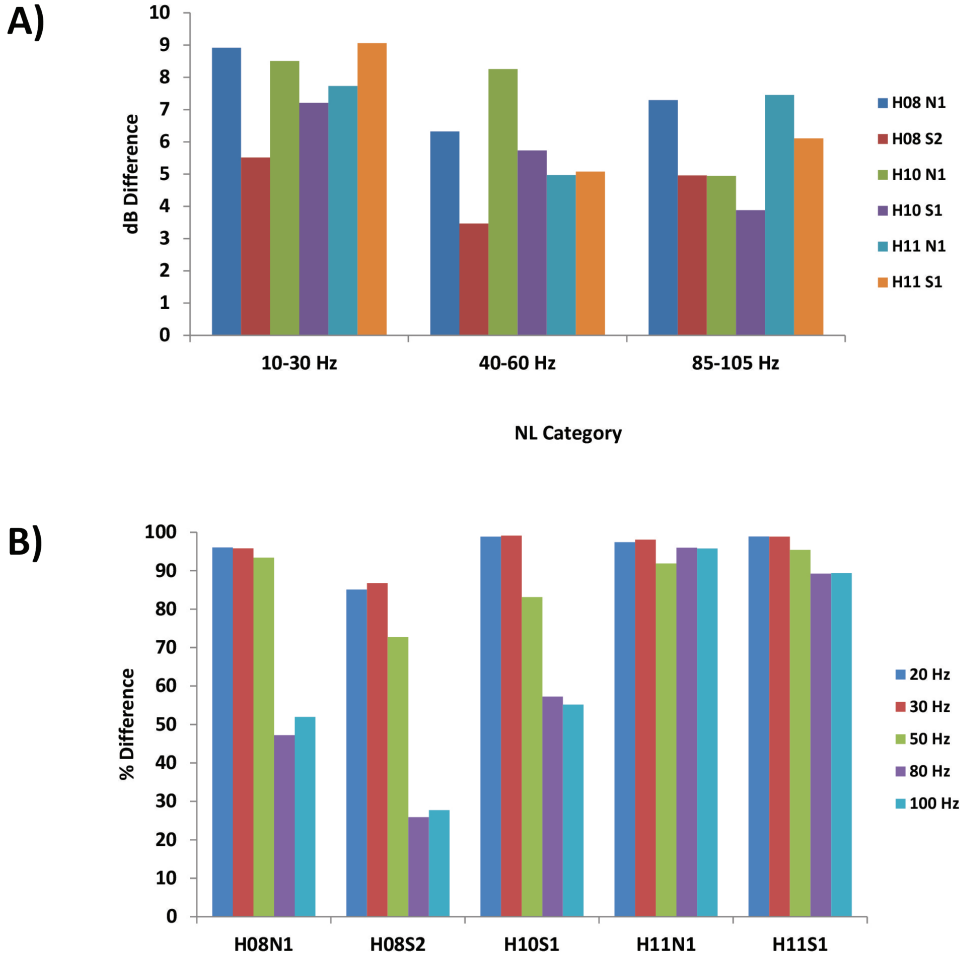

Figure 5. (A) Monthly dB differences over 2 y from 2010-2011 at each location; and (B) corresponding % Difference in estimated signal DA at each location.

frequencies attributed to changes in sound speed alone was less than 15% at H08 Diego Garcia.

The seasonal NL (Figure 3) was reflective of the monthly and daily NL measurements across frequency and location. As this effort focused on the soundscape variability and how it translates into DA variation, the remaining results present dB differences in NL as opposed to absolute levels. The dB difference was defined as the difference between the maximum and minimum NL values at the 5% false alarm rate within each temporal analysis (e.g., the dB differences highlighted in Figure 3 across seasons). The dB differences reflect either seasonal, monthly, or daily differences depending on the time scale of analysis.

Monthly dB differences ranged from 4 to 9 dB across frequency category and location (Figure 5A). The highest and lowest monthly sound levels mimicked the seasonal sound level pattern and directly translated to DA with the largest DAs occurring in months with the lowest sound levels (Figure 4). The greatest NL variability was observed in the 10 to 30 Hz band and translated to variability in the DA estimates (Figure 5B) for which variability was greatest for 20 and 30 Hz signals. Variability in the 80 and 100 Hz propagation was at a minimum at H08 Diego Garcia in the Indian Ocean (26 to 28% difference) and H10 Ascension Island in the Atlantic (55 to 57% difference). The H11 Wake Island location in the Pacific showed the greatest variability in DA across all frequencies (> ~90% difference) (Figure 5B), which is reflective of the > 5 dB difference in NL for all noise bands.

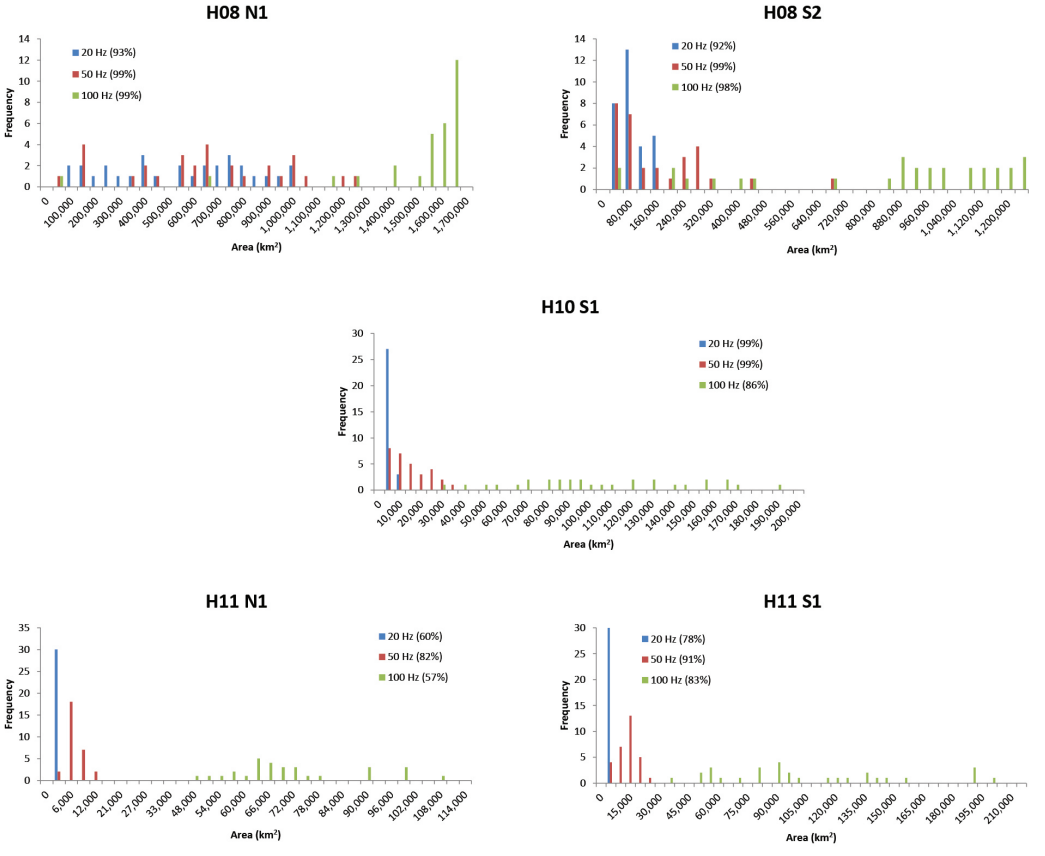

Figure 6. Frequency distribution histograms of daily estimated DA over 30 d in November 2011. The y-axis labels refer to the frequency of daily occurrence, whereas the acoustic frequencies of modelled signals are reflected in the figure legends. The % values in the legends represent the DA % Difference for designated frequencies.

Variability in DA estimates observed at the daily time scale ranged from 45 to 99% difference across frequency and locations (Figure 6). The smallest amount of DA variability (25%) was observed in the 30 Hz DA distribution at H11 N1 Wake Island North. The largest daily differences across frequencies were consistently observed at H08 Diego Garcia. Daily analyses in November 2011 revealed that the distribution of DA estimates differed between locations as a function of frequency (Figure 6). At H08 Diego Garcia, there was a large overlap between the distributions of the DA estimates for 20 and 50 Hz, whereas there was less overlap between the 100 and 50 Hz DA estimates. The DA estimate distribution at H10 Ascension Island was similar to that of H08 S2 Diego Garcia South with the 100 Hz distribution having minimal overlap with the 50 Hz distribution and no correlation with the 20 Hz distribution. The DA estimate distributions at H11 Wake Island were the most disparate with comparatively less variability in the 20 Hz DA estimates and no overlap between the 100 Hz distribution and the 20 or 50 Hz DA estimate distributions.

Discussion

This study addressed differences in DA estimates reflective of changes in the ambient conditions over a season, month, or day and did not address differences in DA as a result of transient sources such as passing vessels. Changes in seasonal sound speed profiles accounted for less than 20% of the modelled DA variability in three different ocean basins, illustrating the critical impact the changing soundscape has on the area that a deep-sea passive acoustic sensor monitors. Order of magnitude differences in DA as a result of changes in the soundscape over time were observed which can translate into a reduction of coverage area by over 90%

as a function of frequency and location, given the stated assumptions about other fixed parameters (e.g., SL). The H08 Indian Ocean location at Diego Garcia had the largest DA of all locations. The modelled area over which blue and fin whales vocalizing at 20 to 30 Hz could be detected shrank by approximately 88% (Figure 4) from summer (850,283 km^2) to winter (106,212 km^2) in 2011 at H08 N1. The accuracy of estimating animal density from PAM data is highly dependent on the survey coverage area (Thomas & Marques, 2012), so being aware of and accounting for this large difference in coverage area would be critical in estimating the density of blue and fin whales. Failure to do so would lead to seasonal biases that could misinform management or risk assessment efforts.

The daily analysis revealed that the three ocean regions examined herein had different soundscape characteristics and, when combined with regional bathymetry, resulted in DA variability patterns that were not uniform across the three locations. Distributions of DA for 20 and 50 Hz signals were essentially the same at H10 Ascension Island and H11 Wake Island and can be considered comparable and separate from the DA distributions of the 100 Hz signal. This was not the case at H08 Diego Garcia in the Indian Ocean where the DA distributions over the same time period overlapped for all modelled frequencies. Results indicate that the different ocean regions have different acoustic characteristics and habitats that require detailed knowledge of the soundscape and bathymetry to determine whether the propagation of multiple low-frequency signals can be considered together or need to be modelled separately.

In order to translate the physical estimates of DA into communication space and masking impacts for vocalizing marine animals, the hearing capabilities related to frequency bands, thresholds, and integration time (processing gain) would need to be combined with SL variability and the physical attributes examined herein (Clark et al., 2009). Linking the physical and biological attributes together to better understand blue and fin whale communication ranges was beyond the scope of this paper. Based on the results of this exercise, it is clear humans who rely on PAM systems for management and mitigation purposes must constantly account for the changing sample areas covered by their sensor or system to accurately interpret source presence at seasonal, monthly, and daily time scales.

Acknowledgments

This work was supported by a Young Investigator Program Award to J. Miksis-Olds from the Office of Naval Research. Thanks are extended to James Neely (AFTAC), Richard Baumstark (AFTAC), Mark Prior (TNO, formerly CTBTO), Andrew Forbes (CTBTO), and Georgios Haralabus (CTBTO) for their assistance in data transfer and transfer of knowledge of CTBTO data.

Literature Cited

Ainslie, M. A. (2010). *Principles of sonar performance modelling*. Berlin: Springer-Verlag. 707 pp.

Amante, C., & Eakins, B. W. (2009). *ETOPO1 1 Arc-Minute Global Relief Model: Procedures, data sources and analysis* (NOAA Technical Memorandum NESDIS NGDC-24). Washington, DC: National Geophysical Data Center, National Oceanic and Atmospheric Administration. http://dx.doi.org/10.7289/V5C8276M

Arveson, P. T., & Vendittis, D. J. (2000). Radiated noise characteristics of a modern cargo ship. *The Journal of the Acoustical Society of America*, *107*, 118-129. http://dx.doi.org/10.1121/1.428344

Boyd, I. L., Frisk, G., Urban, E., Tyack, P., Ausubel, J., Seeyave, S., . . . Shinke, T. (2011). An international quiet ocean experiment. *Oceanography*, *24*, 174-181. http://dx.doi.org/10.5670/oceanog.2011.37

Castellote, M., Clark, C. W., & Lammers, M. O. (2011). Fin whale (*Balaenoptera physalus*) population indemnity in the western Mediterranean Sea. *Marine Mammal Science*, *28*, 325-344. http://dx.doi.org/10.1111/j.1748-7692.2011.00491.x

Clark, C. W., Ellison, W. T., Southall, B. L., Hatch, L., Van Parijs, S. M., Frankel, A., & Ponirakis, D. (2009). Acoustic masking in marine ecosystems: Intuitions, analysis, and implication. *Marine Ecological Progress Series*, *395*, 201-222. http://dx.doi.org/10.3354/meps08402

Collins, M. (1993). A split-step Padé solution for the parabolic equation method. *The Journal of the Acoustical Society of America*, *93*, 1736-1742. http://dx.doi.org/10.1121/1.406739

Heaney, K. D., Kuperman, W. A., & McDonald, B. E. (1991). Perth-Bermuda sound propagation (1960). Adiabatic mode interpretation. *The Journal of the Acoustical Society of America*, *90*(5), 2586-2594. http://dx.doi.org/10.1121/1.402062

Janik, V. M. (2000). Source levels and the estimated active space of bottlenose dolphin (*Tursiops truncatus*) whistles in the Moray Firth, Scotland. *Journal of Comparative Physiology A*, *186*, 673-680. http://dx.doi.org/10.1007/s003590000120

Lawrence, M. W. (2004). Acoustic monitoring of the global ocean for the CTBT. *Proceedings of ACOUSTICS*, *1*, 455-460.

McWilliam, J. N., & Hawkins, A. D. (2013). A comparison of inshore marine soundscapes. *Journal of Experimental Marine Biology and Ecology*, *446*, 166-176. http://dx.doi.org/10.1016/j.jembe.2013.05.012

Mellinger, D. K., Stafford, K. M., Moore, S. E., Dziak, R., & Matsumoto, H. (2007). Fixed passive acoustic observation methods for cetaceans. *Oceanography*, *20*, 36.

Miksis-Olds, J. L., Bradley, D. L., & Niu, X. M. (2013). Decadal trends in Indian Ocean ambient sound. *The Journal of the Acoustical Society of America*, *134*, 3464-3475. http://dx.doi.org/10.1121/1.4821537

Munk, W., Spindel, R., Baggeroer, A., & Birdsall, T. (1994). The Heard Island feasibility test. *The Journal of the Acoustical Society of America*, *96*, 2330. http://dx.doi.org/10.1121/1.410105

Oleson, E. M., Calambokidis, J., Burgess, W. C., McDonald, M. A., LeDuc, C. A., & Hildebrand, J. A. (2007). Behavioral context of call production by eastern North Pacific blue whales. *Marine Ecology Progress Series*, *330*, 269-284.

Pijanowski, B. C., Villaneuva-Rivera, L. J., Dumyahn, S. L., Farina, A., Krause, B. L., Napoletano, B. M., . . . Pieretti, N. (2011). Soundscape ecology: The science of sound in the landscape. *BioScience*, *61*(3), 203-216. http://dx.doi.org/10.1525/bio.2011.61.3.6

Ross, D. (2005). Ship sources of ambient noise. *IEEE Journal of Oceanic Engineering*, *30*, 257-261. http://dx.doi.org/10.1109/JOE.2005.850879

Samaran, F., Adam, O., & Guinet, C. (2010). Detection range modelling of blue whale calls in the southwestern Indian Ocean. *Applied Acoustics*, *71*, 1099-1106. http://dx.doi.org/10.1016/j.apacoust.2010.05.014

Širović, A., Hildebrand, J. A., & Wiggins, S. M. (2007). Blue and fin whale call source levels and propagation range in the Southern Ocean. *The Journal of the Acoustical Society of America*, *122*, 1208-1215. http://dx.doi.org/10.1121.1.2749452

Slabbekoorn, H., & Niels, B. (2008). Soundscape orientation: A new field in need of sound investigation. *Animal Behaviour*, *76*, e5-e8. http://dx.doi.org/10.1016/j.anbehav.2008.06.010

Staaterman, E., Paris, C. B., DeFerrari, H. A., Mann, D. A., Rice, A. N., & D'Alessandro, E. K. (2014). Celestial patterns in marine soundscapes. *Marine Ecology Progress Series*, *508*, 17-32. http://dx.doi.org/10.3354/meps10911

Stafford, K. M., Bohnenstiehl, D. R., Tolstoy, M., Chapp, E., Mellinger, D. K., & Moore, S. E. (2004). Antarctic-type blue whale calls recorded at low latitudes in the Indian and eastern Pacific Oceans. *Deep Research I*, *51*, 1337-1346. http://dx.doi.org/10.1016/j.dsr.2004.05.007

Thomas, L., & Marques, T. A. (2012). Passive acoustic monitoring for estimating animal density. *Acoustics Today*, *8*(3), 35-44.

Tolstoy, M., Diebold, J. B., Webb, S. C., Bohnenstiehl, D. R., Chapp, E., Holmes, R. C., & Rawson, M. (2004). Broadband calibration of *R/V Ewing* seismic sources. *Geophysical Research Letters*, *31*, L14310. http://dx.doi.org/10.1029/2004GL020234

Urick, R. (1967). *Principles of underwater sound*. New York: McGraw-Hill.

Van Opzeeland, I. C., & Miksis-Olds, J. L. (2012). Acoustic ecology of pinnipeds in polar habitats. In D. L. Eder (Ed.), *Aquatic animals: Biology, habitats, and threats* (pp. 1-52). New York: Nova Science Publishers, Inc.

Watkins, W. A., Tyack, P., Moore, K. E., & Bird, J. E. (1987). The 20-Hz signals of finback whales (*Balaenoptera physalus*). *The Journal of the Acoustical Society of America*, *82*, 1901-1912. http://dx.doi.org/0.1121/1.395685

Supplementary Materials

S1. Seasonal detection area (DA) estimates made in 2011; all detection area estimates are given in km^2.

	Frequency	Spring	Summer	Fall	Winter	Range (km^2)	% Difference
H08 N1	20 Hz	261,869	850,283	814,767	106,212	744,071	88
	30 Hz	289,616	704,937	728,916	131,969	596,947	82
	50 Hz	162,322	356,645	624,616	137,082	487,534	78
	80 Hz	1,511,472	1,564,080	1,615,926	1,460,298	155,628	9
	100 Hz	1,528,647	1,536,501	1,569,547	1,420,954	148,593	9
H08 S2	20 Hz	27,758	68,925	45,206	42,978	41,167	59
	30 Hz	30,547	72,860	46,702	48,081	42,313	58
	50 Hz	147,914	177,476	193,375	150,059	45,461	23
	80 Hz	999,221	1,040,265	1,081,784	1,072,914	82,563	7
	100 Hz	992,506	987,621	1,109,136	1,041,877	121,515	10
H10 S1	20 Hz	1,327	5,539	4,054	4,047	4,212	76
	30 Hz	1,229	5,084	3,539	3,382	3,855	76
	50 Hz	20,374	55,052	17,247	19,688	37,805	68
	80 Hz	153,076	215,329	174,472	152,613	62,716	29
	100 Hz	146,675	126,833	166,366	141,553	39,533	23
H11 N1	20 Hz	4,501	2,819	1,464	1,308	3,193	71
	30 Hz	3,887	2,498	1,113	990	2,897	75
	50 Hz	1,818	6,301	3,793	1,041	5,260	83
	80 Hz	18,464	77,463	46,795	16,192	61,271	79
	100 Hz	18,914	69,563	44,432	16,321	53,242	77
H11 NS1	20 Hz	15,624	7,491	2,650	2,667	12,974	83
	30 Hz	13,620	6,968	2,907	2,337	11,283	83
	50 Hz	3,949	13,867	8,393	3,403	10,464	75
	80 Hz	26,815	91,159	61,839	23,825	67,334	74
	100 Hz	24,824	90,899	54,261	23,536	67,363	74

S2. Monthly DA statistics for estimates made from 2010-2011 at each location

	Frequency	Mean (km^2)	SD (km^2)	Range (km^2)	% Difference
H08 N1	20 Hz	518,155	365,980	1,083,061	96
	30 Hz	482,270	320,259	1,056,532	96
	50 Hz	296,097	173,493	633,290	93
	80 Hz	1,471,396	158,839	763,429	47
	100 Hz	1,452,574	169,896	829,748	52
H08 S2	20 Hz	72,400	39,576	143,350	85
	30 Hz	78,772	44,957	175,372	87
	50 Hz	148,967	47,280	178,612	73
	80 Hz	1,017,641	73,087	295,870	26
	100 Hz	1,003,865	77,406	322,362	28
H10 S1	20 Hz	4,593	3,886	17,788	99
	30 Hz	4,055	3,481	15,604	99
	50 Hz	26,126	14,320	46,146	83
	80 Hz	172,932	32,511	142,386	57
	100 Hz	163,413	30,328	127,723	55
H11 N1	20 Hz	3,352	2,370	10,167	97
	30 Hz	3,004	2,635	11,848	98
	50 Hz	4,052	3,249	11,192	92
	80 Hz	44,475	33,445	125,300	96
	100 Hz	40,409	27,706	106,188	96
H11 S1	20 Hz	6,103	4,895	16,484	99
	30 Hz	5,626	4,325	15,134	99
	50 Hz	8,032	5,798	16,422	95
	80 Hz	53,686	37,420	151,955	89
	100 Hz	50,196	35,046	146,212	89

S3. Daily DA statistics for estimates made in November 2011 at each location

	Frequency	Mean (km²)	SD (km²)	Range (km²)	% Difference
H08 N1	20 Hz	526,265	281,258	917,327	93
	30 Hz	480,292	249,311	830,764	92
	50 Hz	617,211	324,861	1,210,411	99
	80 Hz	1,504,348	345,500	1,667,895	99
	100 Hz	1,459,215	341,476	1,620,458	99
H08 S2	20 Hz	67,913	40,713	140,033	92
	30 Hz	70,543	42,391	146,659	93
	50 Hz	148,279	145,168	657,901	99
	80 Hz	785,166	378,270	1,158,351	98
	100 Hz	801,992	386,574	1,188,851	98
H10 S1	20 Hz	2,109	2,330	8,307	99
	30 Hz	1,831	2,115	7,603	99
	50 Hz	11,979	8,815	32,864	99
	80 Hz	109,904	44,227	169,070	86
	100 Hz	103,524	41,539	159,659	86
H11 N1	20 Hz	1,083	228	816	60
	30 Hz	915	93	487	45
	50 Hz	5,405	2,308	10,045	82
	80 Hz	79,812	16,795	69,072	58
	100 Hz	70,497	15,215	60,220	57
H11 S1	20 Hz	1,554	404	1,847	78
	30 Hz	1,366	410	1,798	78
	50 Hz	11,252	5,142	21,064	91
	80 Hz	114,042	49,906	177,613	83
	100 Hz	102,315	45,910	161,751	83